

Supplementary Materials for  
**Ibrutinib Inhibition of ERBB4 Reduces Cell Growth in a WNT5A  
Dependent Manner**

Femina Rauf <sup>1</sup>, Fernanda Festa<sup>1</sup>, Jin G Park<sup>1</sup>, Mitchell Magee<sup>1</sup>, Seron Eaton<sup>1</sup>,  
Capria Rinaldi<sup>1</sup>, Carlos Morales Betanzos<sup>1</sup>, Laura Gonzalez-Malerva<sup>1</sup>, and  
Joshua LaBaer<sup>1\*</sup>

Correspondence to: [jlabaer@asu.edu](mailto:jlabaer@asu.edu)

**This PDF file includes:**

Figs. S1 to S17

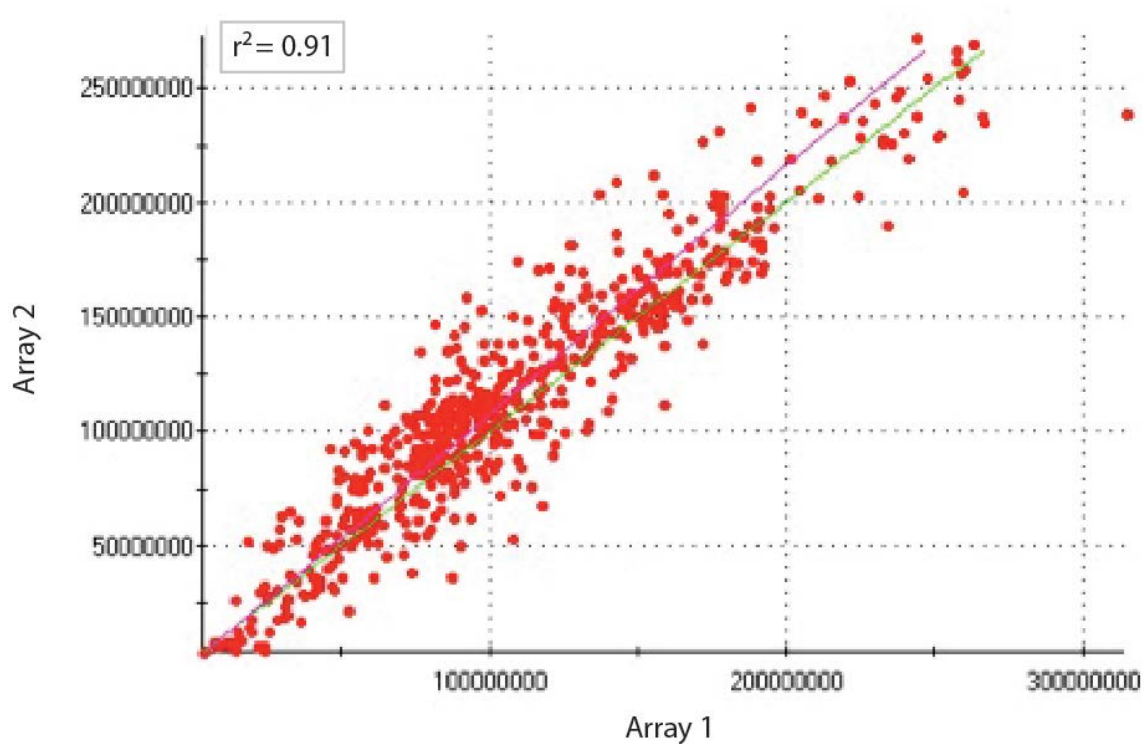


**Fig. S1.**  
**Correlation of protein display in NAPPA-kinase arrays.** Correlation plot between two NAPPA kinase arrays printed in the same batch. Array 1 corresponds to a slide printed early in the batch while Array 2 was printed later from the same batch.

## Staurosporine screening on NAPPA kinase array

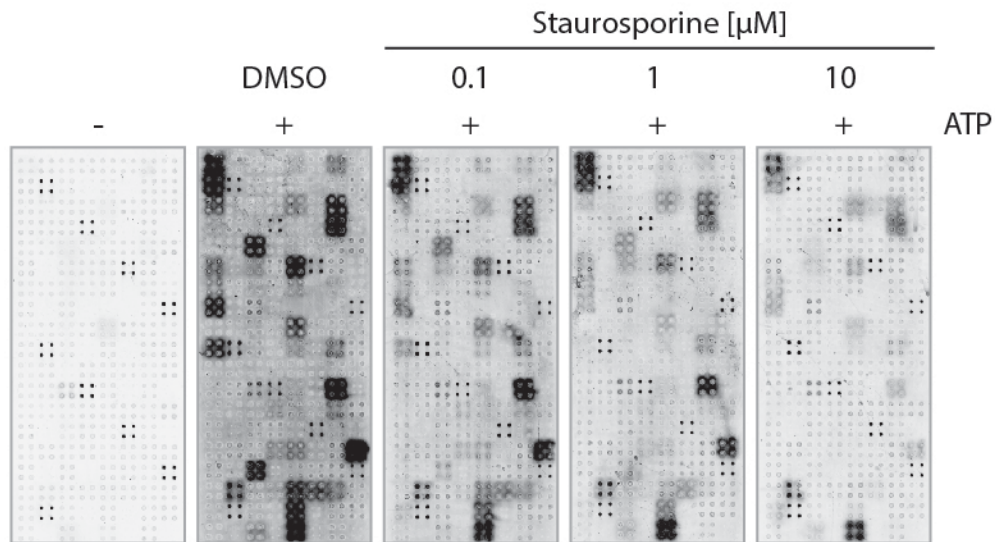


**Fig. S2.**

**Staurosporine screening in NAPPA kinase arrays.** Dephosphorylated NAPPA kinase arrays were incubated with staurosporine at concentrations ranging from 0.1  $\mu\text{M}$  to 10  $\mu\text{M}$  during the autophosphorylation reaction. DMSO was used as vehicle and control. The phosphorylation levels were measured with anti-pTyr. Representative array images of protein phosphorylation after the autophosphorylation reaction is shown.

## Ibrutinib screening on NAPPA kinase array

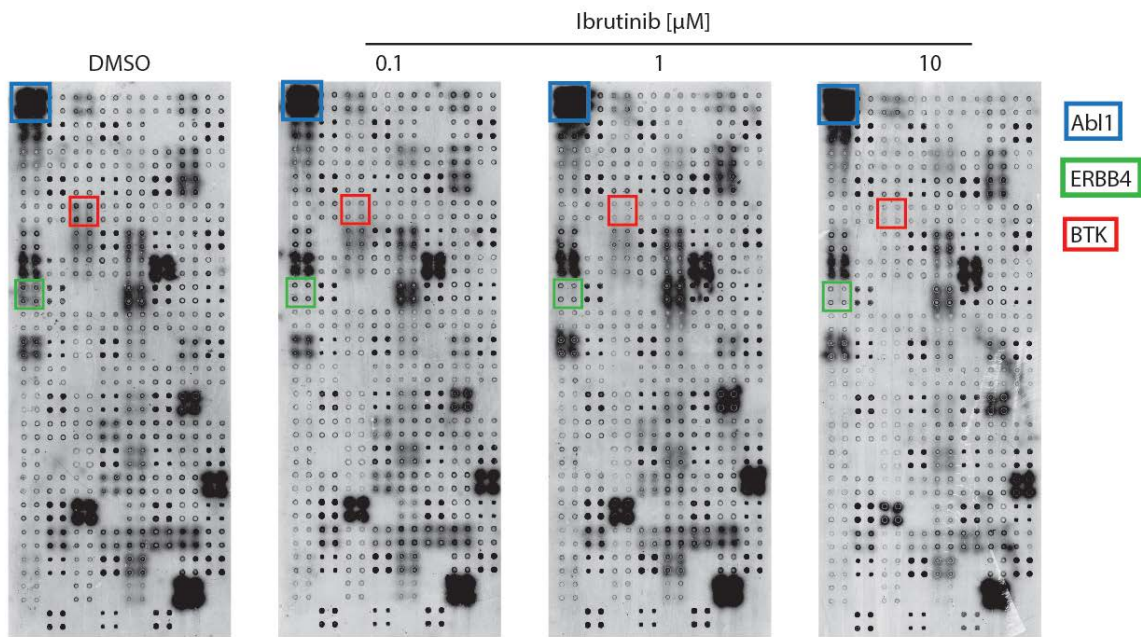


**Fig. S3.** Ibrutinib screening in NAPPA kinase arrays. Dephosphorylated NAPPA kinase arrays were incubated with ibrutinib at concentrations ranging from 0.1  $\mu\text{M}$  to 10  $\mu\text{M}$  during the autophosphorylation reaction. DMSO was used as vehicle and control. The phosphorylation levels were measured with anti-pTyr. Representative array images showing protein phosphorylation after the autophosphorylation reaction is shown.

## Radioactive kinase assay in the presence of Ibrutinib

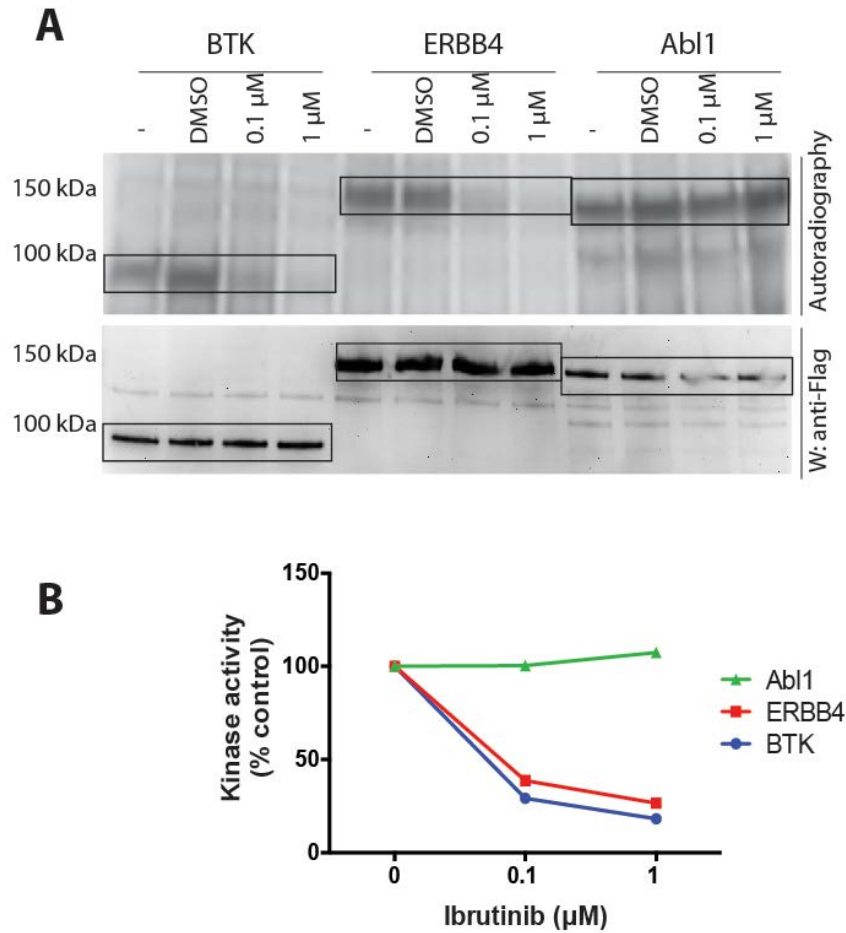


**Fig. S4.**

**Ibrutinib inhibits ERBB4 in solution.** Radioactive kinase assay was performed *in vitro* using purified BTK, ERBB4 and ABL1 proteins. (A) Autoradiography shows the effect of ibrutinib in the autophosphorylation levels of each kinase. The expected band for each protein is shown inside the box. (B) Quantification of kinase activity obtained in the radioactive kinase assay.

## Selection of cell lines expressing high levels of ERBB4

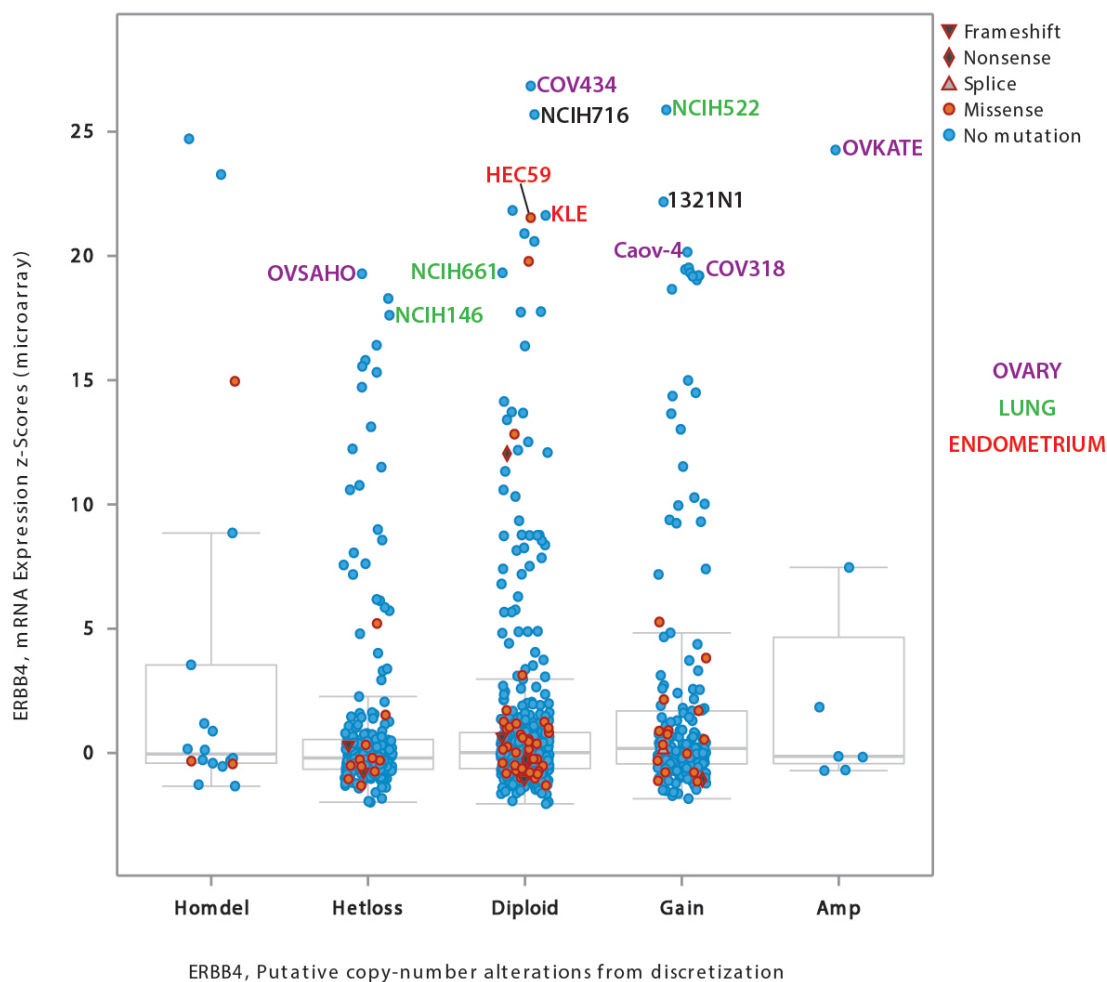


**Fig. S5.**  
**Selection of human cell lines overexpressing ERBB4.** Microarray data from the Cancer Cell Line Encyclopedia available at cBioPortal for Cancer Genomics was used for the selection of cancer cell lines overexpressing ERBB4. A total of 11 cell lines were chosen. Their ERBB4 levels and the tissue of origin are shown. Cells labeled in purple are from ovarian cancer, cells labeled in green are from lung cancer and cells labeled in red are from endometrium cancer.

## ERBB4 and BTK levels

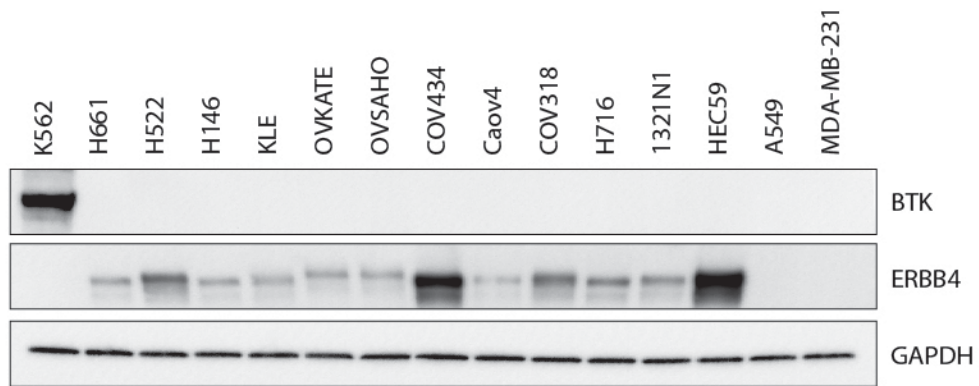


**Fig. S6.**

**Cell line characterization.** Protein levels of ERBB4 and BTK were measured in ERBB4<sup>High</sup>/BTK<sup>Low</sup> cell lines (H146, 1321N1, COV318, Caov4, COV434, HEC59, OVSAHO, OVKATE, H522, H661, KLE, H716), and ERBB4<sup>Low</sup>/BTK<sup>Low</sup> cell lines (MDA-MB-231 and A549). The cell line K562 was used as a positive control for BTK and GAPDH was used as a loading control for all the samples.

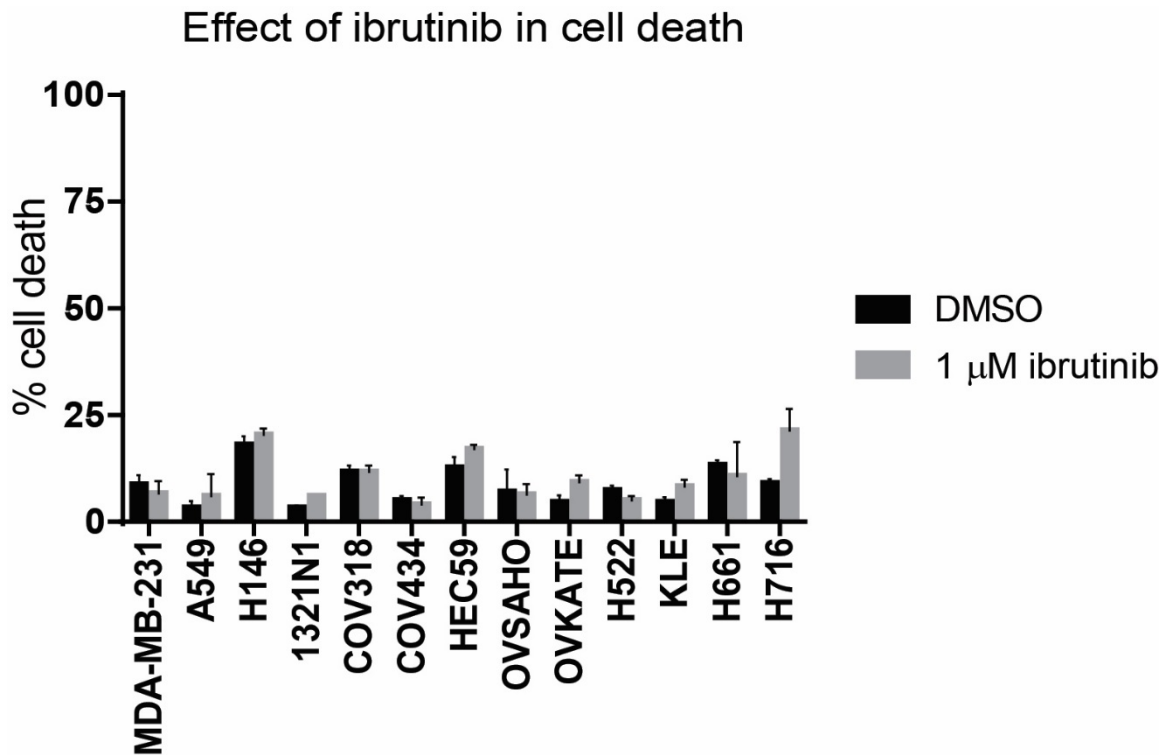


**Fig. S7.**  
**Effect of ibrutinib in cell death.** Cell death was monitored in ERBB4<sup>High</sup>/BTK<sup>Low</sup> and ERBB4<sup>Low</sup>/BTK<sup>Low</sup> cell lines after ibrutinib treatment (6 days, 1  $\mu$ M). The number of dead cells is reported as a percentage along with the DMSO treated control.

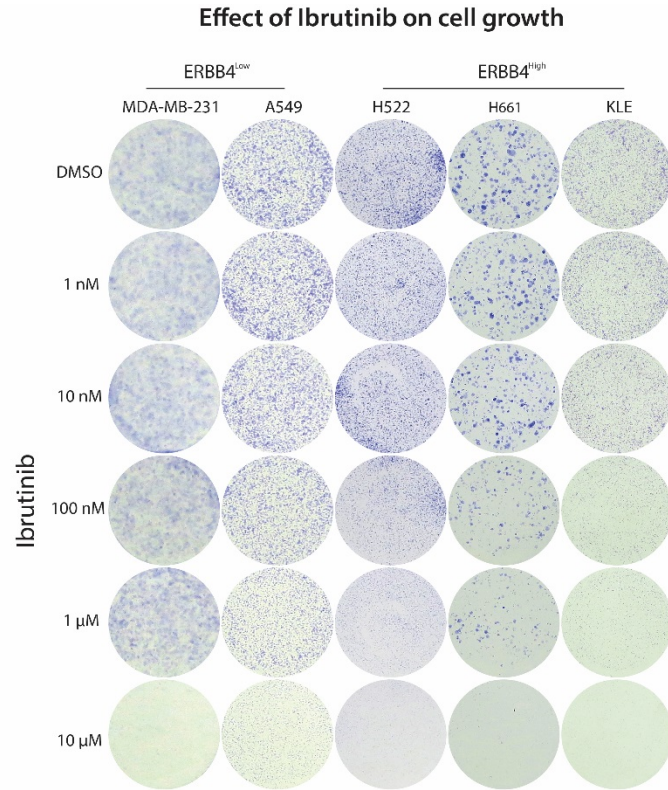


**Fig. S8.**

**Ibrutinib effect on cell proliferation.** Microscopic view of crystal violet-stained ERBB4<sup>Low</sup>/BTK<sup>Low</sup> cells (A549 and MDA-MB-231) and ERBB4<sup>high</sup>/BTK<sup>Low</sup> cells (H522, H661 and KLE) after 6 days of ibrutinib treatment.

## Ibrutinib response in EGFR and ERBB2 knockdown H661 cells

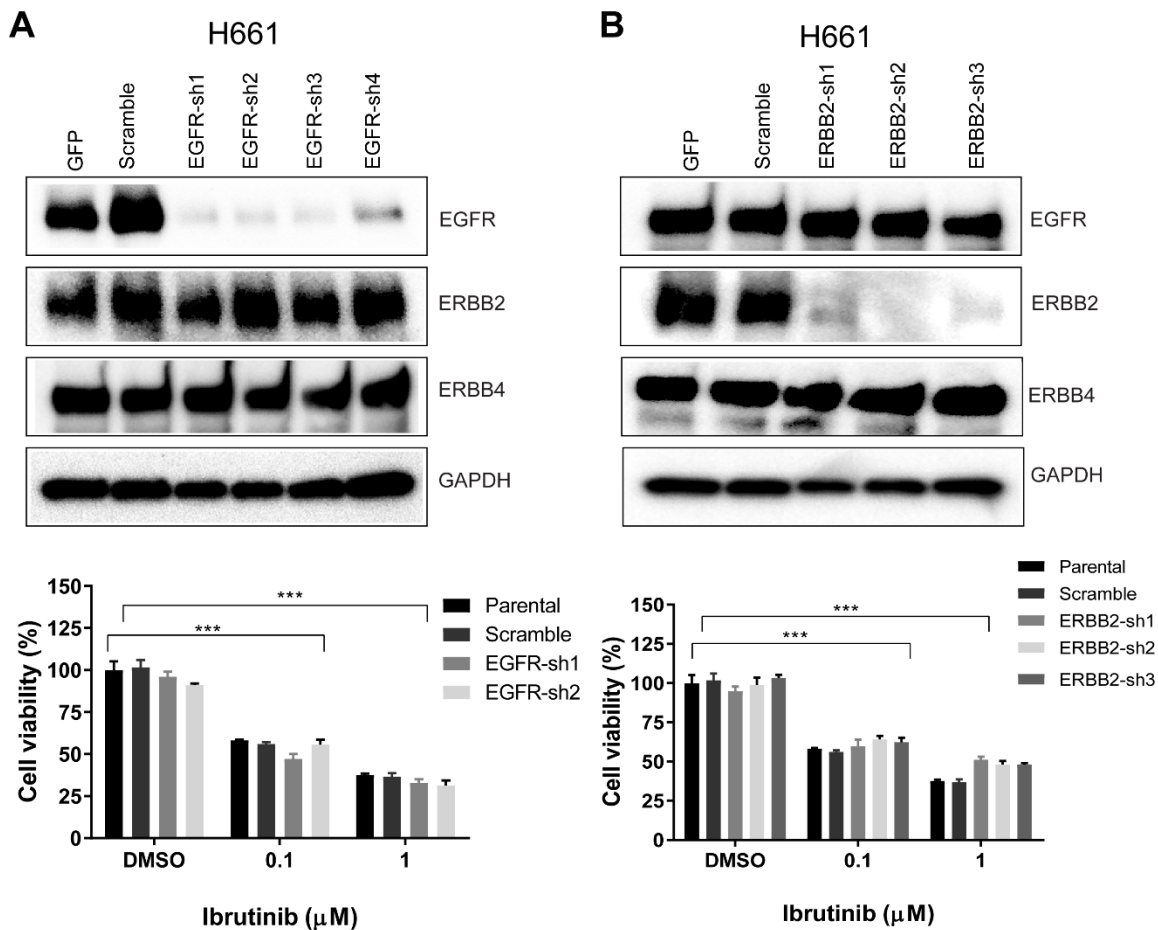


**Fig. S9.**

**Ibrutinib response in EGFR and ERBB2 knock-down H661 cells.** (A) Western blot for EGFR, ERBB2, ERBB4 and GAPDH in H661 cells infected with shRNAs against EGFR, GFP and scramble along with cell proliferation after ibrutinib treatment (6 days, 0.1-1  $\mu\text{M}$ ). (B) Western blot for EGFR, ERBB2, ERBB4 and GAPDH in H661 cells infected with shRNAs against ERBB2, GFP and scramble along with cell proliferation after ibrutinib treatment (6 days, 0.1-1  $\mu\text{M}$ ). Data are reported as mean  $\pm$  s.e.m with  $n=3$  (\*\*\*)  $P < 0.001$ .

## Ibrutinib response in EGFR and ERBB2 knockdown KLE cells

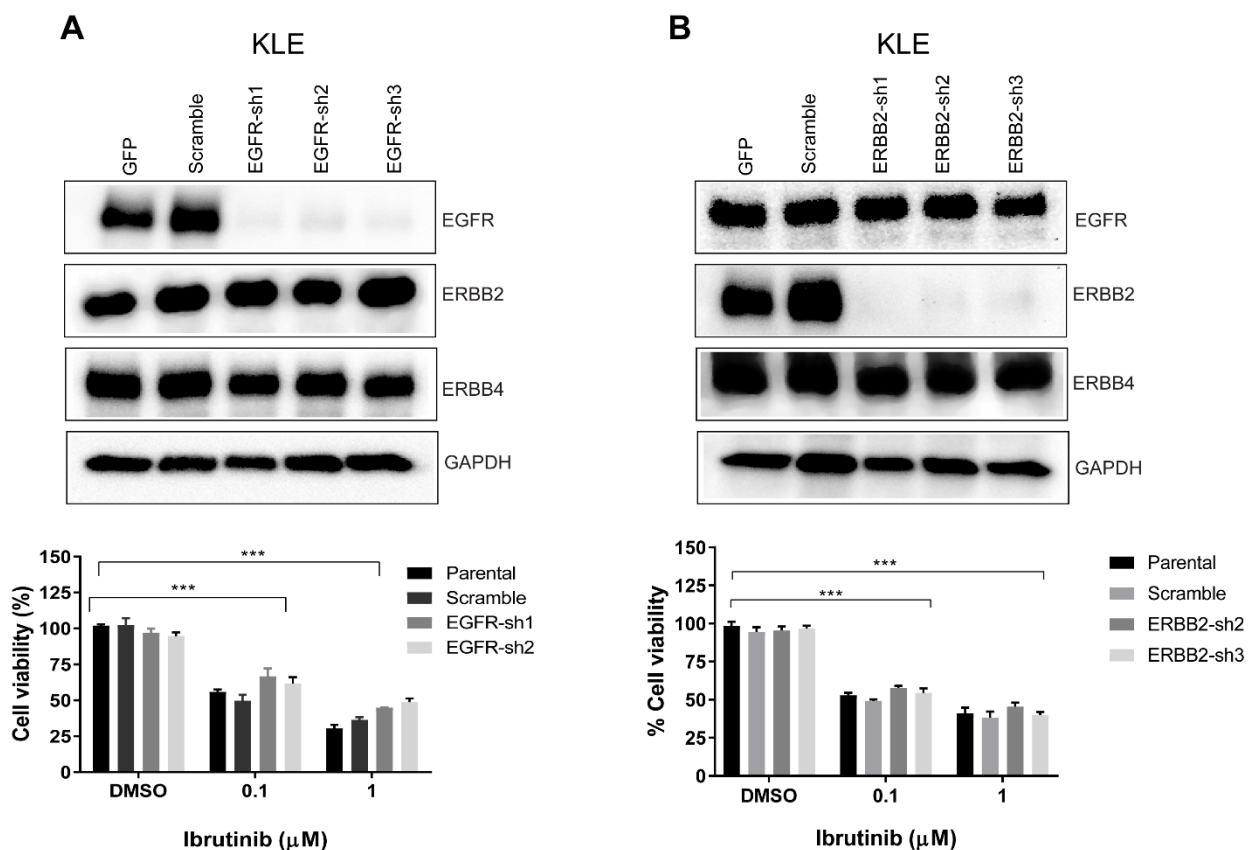


**Fig. S10.**

**Ibrutinib response in EGFR and ERBB2 knock-down KLE cells.** (A) Western blot for EGFR, ERBB2, ERBB4 and GAPDH in KLE cells infected with shRNAs against EGFR, GFP and scramble along with cell proliferation after ibrutinib treatment (6 days, 0.1-1  $\mu\text{M}$ ). (B) Western blot for EGFR, ERBB2, ERBB4 and GAPDH in KLE cells infected with shRNAs against ERBB2, GFP and scramble along with cell proliferation after ibrutinib treatment (6 days, 0.1-1  $\mu\text{M}$ ). Data are reported as mean  $\pm$  s.e.m with  $n=3$  (\*\*\*)  $P < 0.001$ .

## Effect of ibrutinib treatment on ERBB4 signaling in EGFR and ERBB2 knockdown KLE and H661 cells

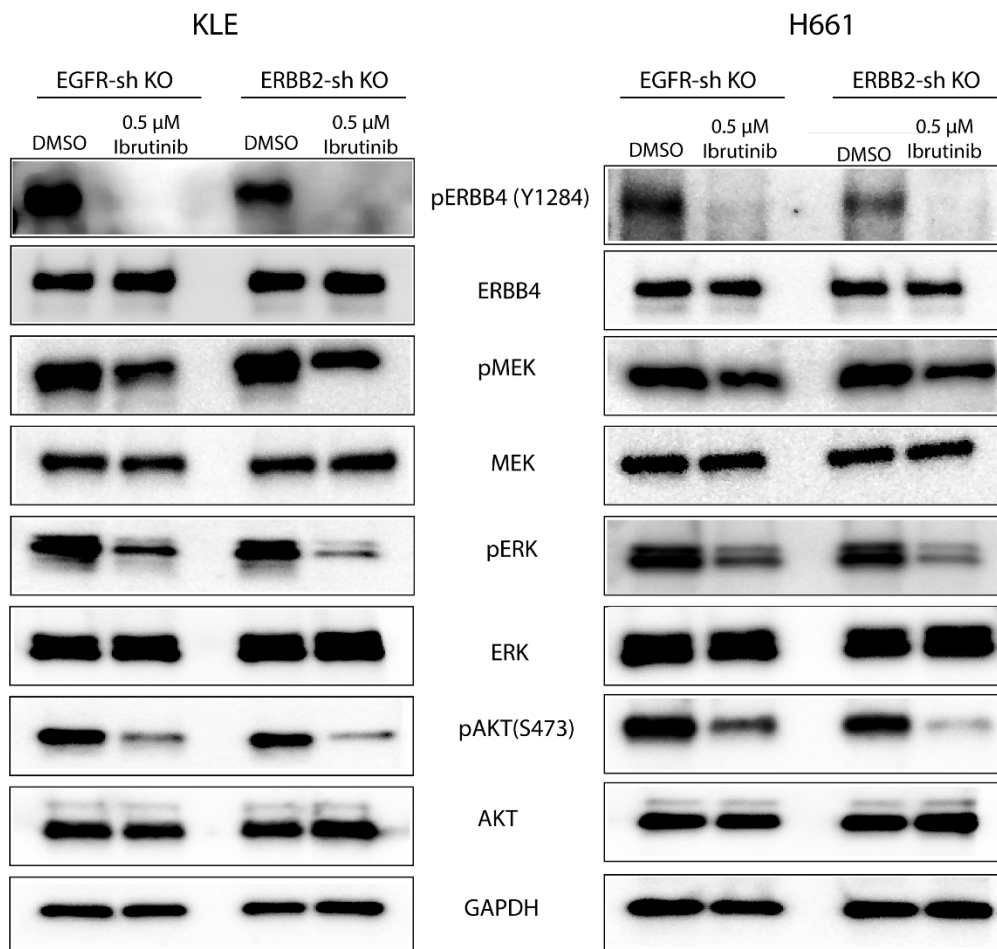


**Fig. S11.**

**Effect of ibrutinib treatment on ERBB4 signaling in EGFR and ERBB2-knocked down KLE and H661 cells.** (A) Western blot for pERBB4, ERBB4, pMEK4, MEK, pERK, ERK, pAKT and AKT in EGFR and ERBB2 knockdown KLE cells after ibrutinib treatment (24 h, 0.5 μM). (B) Western blot for pERBB4, ERBB4, pMEK4, MEK, pERK, ERK, pAKT and AKT in EGFR and ERBB2 knockdown H661 cells after ibrutinib treatment (24 h, 0.5 μM).

## Tumor growth of ibrutinib responsive and non-responsive cell-derived mouse xenografts

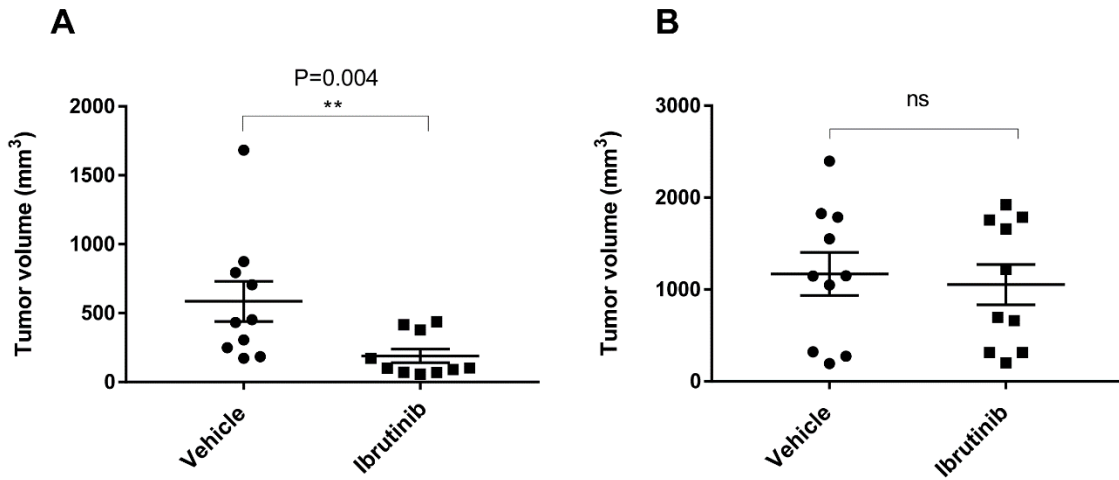


**Fig. S12.**

**Effect of ibrutinib treatment on H661 and 1321N1 cell-derived mouse xenografts.** (A) Tumor growth of H661 cell-derived mouse xenografts (n=10) after daily treatment of ibrutinib (1mg/Kg) and buffer only control. (B) Tumor growth of 1321N1 cell-derived mouse xenografts (n=10) after daily treatment of ibrutinib (5mg/Kg) and buffer only control.

## Protein levels of ERBB4 and pERBB4

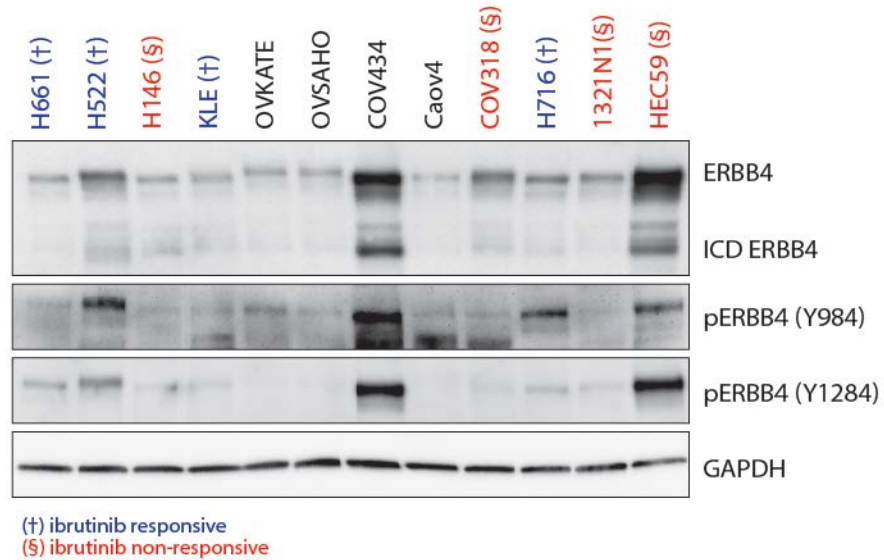


**Fig. S13.**

**Levels of phospho-ERBB4 and ICD ERBB4.** Western blot analysis for ERBB4, pERBB4 (Y984) and pERBB4 (Y1284) was performed in ERBB4<sup>High</sup>/BTK<sup>Low</sup> cell lines H146, 1321N1, COV318, Caov4, COV434, HEC59, OVSAHO, OVKATE, H522, H661, KLE, H716. GAPDH was used as control.

## Protein levels of EGFR family members

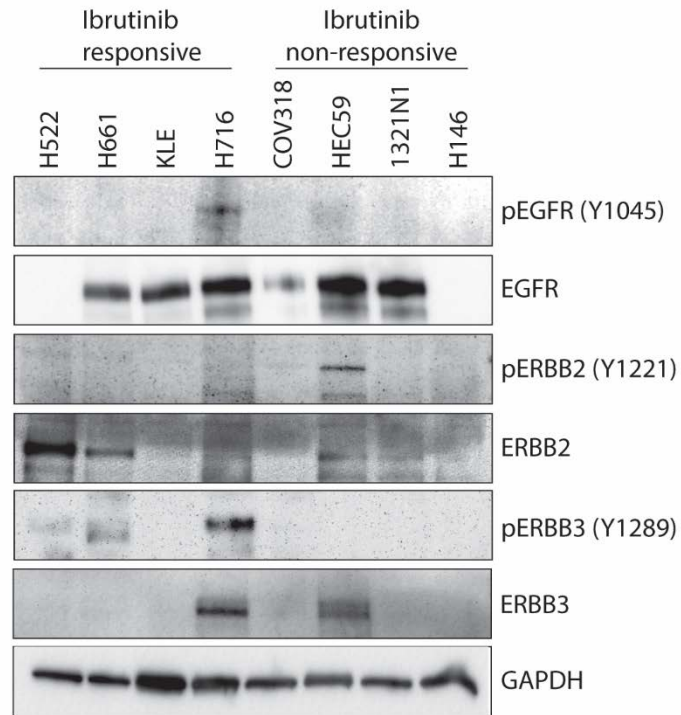


**Fig. S14.**

**Characterization of EGFR family members in ibrutinib responsive and non-responsive cell lines.** Western blot for pEGFR (Y1045), EGFR, pERBB2 (Y1221), ERBB2, pERBB3 (Y1289), ERBB3 and GAPDH was performed in ibrutinib responsive (H522, H661, KLE, H716) and non-responsive cell lines (COV318, HEC59, 1321N1, H146).

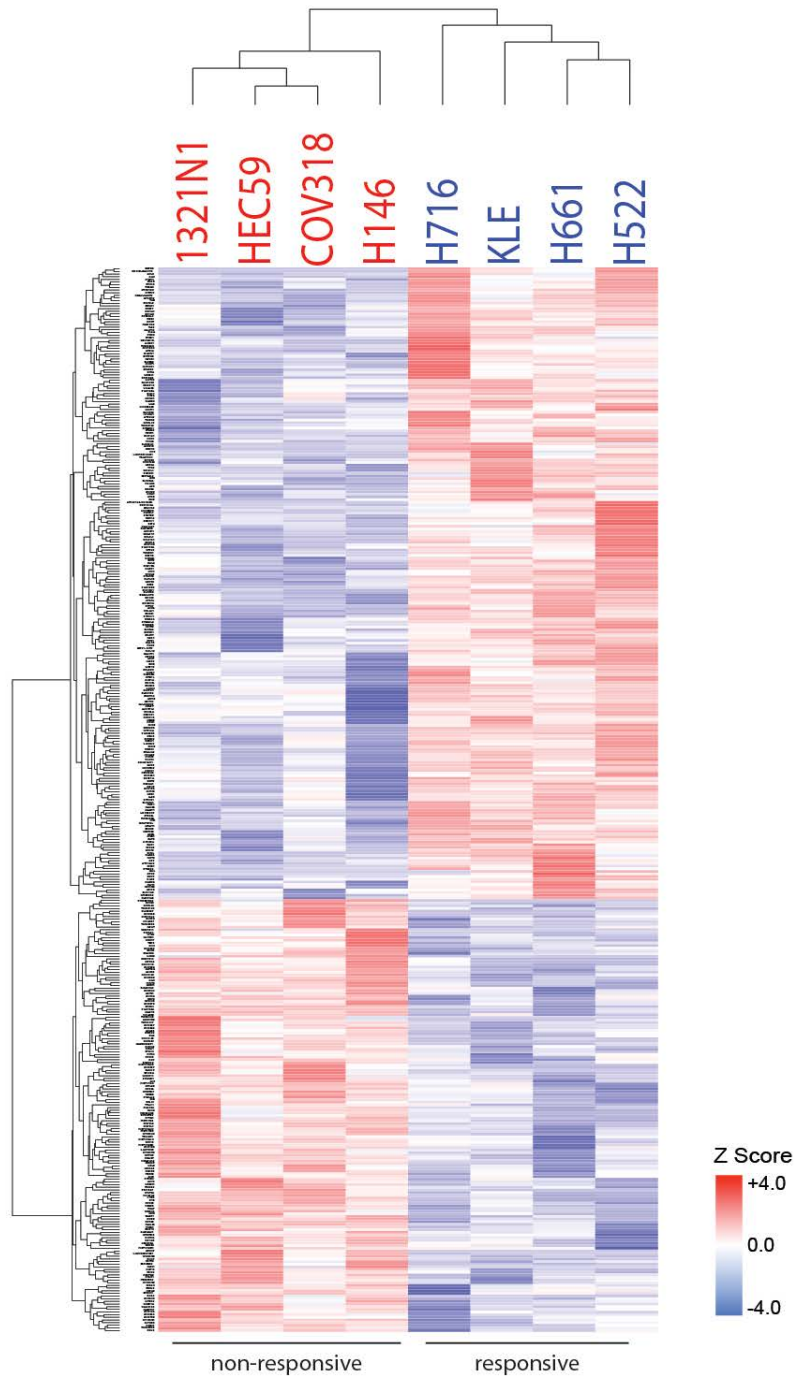


**Fig. S15.** Heat map of hierarchical clustering of 401 genes differentially expressed between ibrutinib responsive (in blue) and non-responsive (in red) cell lines.

## Effect of Ibrutinib on cell growth

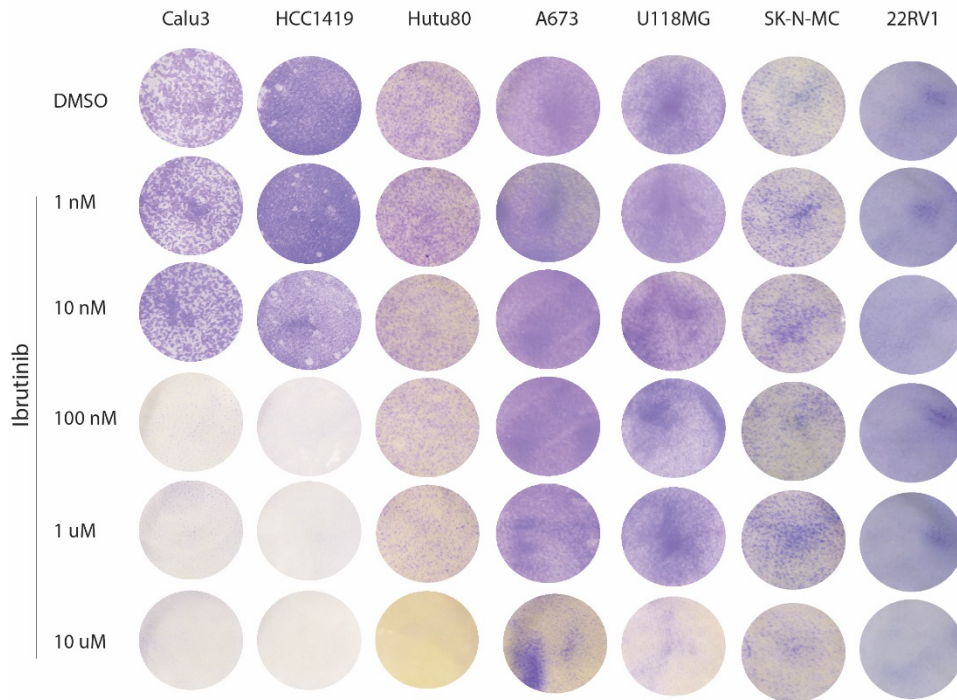


**Fig. S16.**

**Ibrutinib effect on ERBB4<sup>High</sup>/BTK<sup>Low</sup> cells with low or high DKK/WNT5A ratio.**

Microscopic view of crystal violet-stained ERBB4<sup>High</sup>/BTK<sup>Low</sup> cells with high

DKK1/WNT5A ratio (Calu-3, HCC1419, HuTu80 and 22RV1) or low DKK1/WNT5A ratio

(SK-N-MC, A673, U-118 MG) after 6 days of ibrutinib treatment.

## Effect of WNT5A on ibrutinib resistance

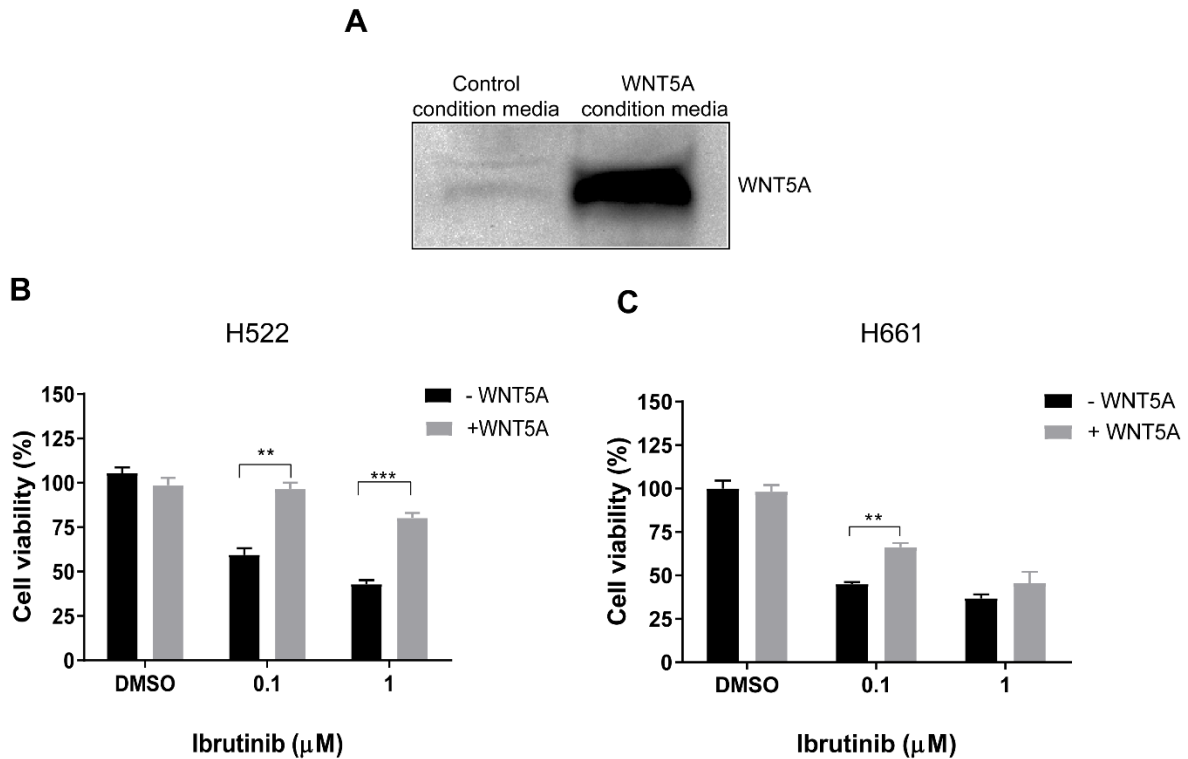


**Fig. S17.**

**Effect of WNT5A on ibrutinib resistance.** (A) Western blot analysis for WNT5A secretion in L Wnt5a secreting cells compared to control L cells. (B) Effect of ibrutinib on cell proliferation in H522 cells in the presence of WNT5A. (C) Effect of ibrutinib on cell proliferation in H661 cells in the presence of WNT5A. Data are reported as mean  $\pm$  s.e.m with  $n=3$  (\*\* $P < 0.002$ \*\*\* $P < 0.001$ ).